

BiP (GRP78) and Endoplasmin (GRP94) Are Induced following Rotavirus Infection and Bind Transiently to an Endoplasmic Reticulum-Localized Virion Component

AIMIN XU, A. RICHARD BELLAMY, AND JOHN A. TAYLOR*

*Biochemistry and Molecular Biology Research Group, School of Biological Sciences,
University of Auckland, Auckland, New Zealand*

Received 7 July 1998/Accepted 7 September 1998

Rotavirus infection induces profound alterations in the morphology and biochemistry of the host cell. Using two-dimensional (2D) gel electrophoresis combined with metabolic labeling, we have identified four proteins that are specifically upregulated in rotavirus-infected cells. Two of these have been identified as BiP (GRP78) and endoplasmin (GRP94), members of a family of glucose-regulated chaperone proteins that reside in the endoplasmic reticulum (ER) lumen, the site of rotavirus morphogenesis. The level of mRNA and the transcriptional activity of the BiP and endoplasmin genes are increased markedly in rotavirus-infected cells, and these genes are also induced when a single rotavirus protein, the nonstructural glycoprotein NSP4, is expressed in MA104 cells. However, NSP4 does not associate with either BiP or endoplasmin, implying that the mechanism of BiP and endoplasmin gene activation by NSP4 may differ from that triggered by viral membrane glycoproteins of other viruses. The interaction of BiP and endoplasmin with rotavirus structural polypeptides suggests that these chaperones are involved in the process of viral maturation in the ER lumen.

Rotaviruses are nonenveloped, triple-layered icosahedral viruses with a genome of 11 segments of double-stranded RNA encoding six structural and five nonstructural polypeptides (11). These viruses have a unique mode of assembly involving specialized viroplasmic inclusions located adjacent to the ER. In the final stages of maturation, the immature inner capsid particle (ICP) is transferred across the membrane of the ER by a budding event initiated when the ICP interacts with a viral nonstructural glycoprotein, NSP4 (1, 23). During and after transfer to the ER lumen, the ICP is enveloped transiently in a membrane vesicle and the outer shell proteins VP7 and VP4 are assembled onto the surface of the particle. The precise details of how infectious virions are assembled within the ER lumen are poorly understood. Little is known about the requirement for the involvement of host proteins in this process, although several studies have demonstrated that a high concentration of Ca^{2+} within the ER lumen is necessary for productive assembly of virions (24, 25, 30).

Rotavirus exhibits a distinctive cytopathic effect characterized by a dramatic reduction in host cell gene expression (8, 10), elevated intracellular levels of calcium (24, 25), and, ultimately, lysis of the infected cell. The cytopathic effect is thought to derive from expression of a viral protein, and recent studies implicate NSP4 as the viral protein responsible. Expression of NSP4 demonstrated that this protein can raise intracellular levels of calcium in insect cells (37, 38) and leads to a loss of plasma membrane integrity and altered nuclear morphology in MA104 cells (28). An additional function recently attributed to NSP4 is that of a viral enterotoxin. Purified NSP4, or a synthetic peptide which represents residues 114 to 135, causes diarrhea in infant mice (2). It is not clear how NSP4 is released from the ER membranes of infected cells to fulfill this postulated role.

Few studies have addressed the issue of how host cells might respond to rotavirus in terms of altered gene expression or enzyme activity. A better knowledge of how the host cell responds to infection might shed light on the mechanism(s) of rotavirus assembly or cytopathogenesis. In this study, we have employed a proteome-mapping approach using two-dimensional (2D) gel electrophoresis to generate a difference map of proteins expressed in mock- and rotavirus-infected MA104 cells. Following infection, at least four host proteins are upregulated, and we have identified two of these as BiP (GRP78) and endoplasmin (GRP94). Furthermore, the transcriptional activity of the genes encoding these proteins has been analyzed, and a possible role for the upregulated proteins in rotavirus assembly has been suggested.

MATERIALS AND METHODS

Cells and viruses. The rhesus monkey kidney cell line MA104 was grown in 199 medium (Gibco) supplemented with 10% tryptose phosphate and 10% newborn calf serum. The SA11 strain of rotavirus was purified and the titer was determined as previously described (35). Reovirus type 3 (Dearing strain) was obtained from W. K. Joklik (Duke University, Durham, N.C.). Vaccinia virus VTF7.3, which expresses T7 RNA polymerase, was kindly provided by B. Moss (National Institutes of Health, Bethesda, Md.). Construction of the recombinant vaccinia virus vTMNSP4, which expresses NSP4 from the SA11 strain of rotavirus (5), has been described elsewhere (28). Prior to infection, rotavirus inocula were activated by addition of 10 μ g of trypsin per ml and incubated at 37°C for 30 min. The virus was added to confluent MA104 cells at 10 PFU/cell in the presence of trypsin. After 3 h, the inoculum was removed and replaced by medium lacking trypsin.

Radiolabeling and immunoprecipitation. Cells were washed twice with Dulbecco's minimal essential medium (DMEM) (Gibco) lacking methionine and cysteine and incubated for 20 min in this medium. The cells were then radiolabeled with 50 μ Ci of Trans-label (ICN) per ml in methionine and cysteine-free DMEM for 16 to 24 h in the case of prelabeled cells (i.e., labeled prior to virus infection) or for 7 h following virus infection. For pulse-labeling studies, cells were labeled at the indicated times for 10 min (unless otherwise stated), after which the medium was removed and replaced with DMEM containing a 20-fold molar excess of unlabeled cysteine and methionine. Cells were harvested with a rubber policeman and centrifuged at 1,000 \times g for 5 min. Cell pellets were stored at -80°C until required. To immunoprecipitate specific proteins, cell pellets were solubilized in 1 ml of lysis buffer (2% CHAPS {3-(cholamidopropyl)-dimethyl-ammonio}-1-propanesulfonate}, 50 mM HEPES [pH 7.5], 200 mM NaCl, 2 mM phenylmethylsulfonyl fluoride (PMSF), 10 U of aprotinin per ml) for

* Corresponding author. Mailing address: School of Biological Sciences, University of Auckland, Private Bag 92019, Auckland, New Zealand. Phone: 64 9 373 7599, ext. 7235. Fax: 64 9 373 7414. E-mail: ja.taylor@auckland.ac.nz.

30 min, and debris was removed by microcentrifugation. Immune complexes were formed by shaking the clarified cell lysate with specific antisera overnight at 4°C and recovered following addition of protein A-Sepharose for 30 min. Beads were washed three times in lysis buffer, and bound proteins were removed by boiling in sodium dodecyl sulfate (SDS) sample buffer prior to electrophoresis.

Preparation of cell lysates and analytical 2D gel electrophoresis. Frozen cell pellets were lysed by incubation in lysis buffer (8 M urea, 4% CHAPS {3-[(3-cholamidopropyl)-dimethyl-ammonio]-1-propanesulfonate}, 2% dithiothreitol [DTT], 2% Pharmalyte 3-10 [Pharmacia], 2 mM PMSF, 2 mM Pefabloc [Boehringer]) for 30 min at room temperature. Lysates were microcentrifuged at 12,000 rpm for 5 min to remove nucleic acid, and the protein concentration of the supernatant was determined in a dye-binding assay with Bradford reagent. Eighty-microgram aliquots of protein were focused on an Immobiline Drystrip 3-10 NL gel (Pharmacia) by using a Multiphor RII electrophoresis system (Pharmacia) with the following voltage program: 5 h to 500 V, 5 h to 3,500 V, and 10 h at 3,500 V at 1 mA. After separation in the first dimension, the Immobiline strips were equilibrated for 10 min in a buffer containing 50 mM Tris HCl (pH 6.8), 8 M urea, 30% glycerol, 1% SDS, and 1% DTT followed by a further 10 min in the same buffer containing 2.5% iodoacetamide. The strips were then laid atop precast 12 to 14% gradient gels for separation of polypeptides in the second dimension. Following electrophoresis, the gels were fixed in 10% glacial acetic acid–20% ethanol, and the proteins were visualized by silver staining and/or by autoradiography at –80°C. Gels were scanned with a Sharp JX325 scanner, and the protein spots were analyzed with Imagemaster software (Pharmacia).

Characterization of proteins by microsequencing and MALDI-TOF MS. Protein spots of interest were excised from Coomassie brilliant blue-stained preparative gels loaded with 800 µg of protein. Gel pieces were subjected to in-gel trypsin digestion as described by Rosenfeld et al. (34). The extracted peptide mixture was fractionated by reverse-phase high-performance liquid chromatography (HPLC) on a Brownlee RP300 C₁₈ column. Fractions were stored at –20°C prior to sequencing. For matrix-assisted laser desorption time-of-flight mass spectrometry (MALDI-TOF MS), a modified protocol for in-gel trypsinization was employed. Briefly, the spots were excised from the gel, cut into <1-mm² pieces, and transferred to 0.5-ml microcentrifuge tubes. Gel pieces were washed twice in 50 mM ammonium bicarbonate in 50% acetonitrile at 30°C for 20 min with shaking. Proteins were reduced by incubation in 10 mM DTT–50 mM ammonium bicarbonate for 1 h, and cysteine residues were carboxymethylated with 25 mM iodoacetamide in 50 mM ammonium bicarbonate for a further hour at room temperature. The buffer was aspirated, and the gel pieces were washed as described above, dried, and digested with trypsin. The peptide mixture was dried and redissolved in 20 to 100 µl of 0.1% trifluoroacetic acid. Two-microliter aliquots were mixed with an equal amount of α-cyano-4-hydroxycinnamic acid, and the samples were vacuum crystallized by using the sample preparation accessory (Hewlett-Packard). Crystals were carefully observed to ensure that crystal formation occurred evenly. The ion-accelerating potential was 30 kV. The MALDI mass spectrum of the peptide mixture was then obtained on a G2025A MALDI-TOF mass spectrometer (Hewlett-Packard).

Analysis of mRNA abundance and transcription activity. Cytoplasmic RNA was isolated from rotavirus-, reovirus-, vaccinia virus-, or mock-infected MA104 cells by using Trizol (Life Technology, Inc.). Total RNA (10 µg) was resolved by electrophoresis on a 1.2% agarose gel containing 2.2 M formaldehyde. The RNA was transferred to a nylon membrane overnight and baked at 80°C for 2 h. Plasmids p3C5 (15) and p4A3 (32), containing the mouse BiP and endoplasmic genes, respectively, were labeled with [α-³²P]dCTP by a random primer method. The membranes were preincubated with hybridization buffer (1 mM EDTA, 40 mM Na₂HPO₄ [pH 7.2], 5% SDS) for 1 h at 65°C and subsequently incubated overnight in fresh buffer containing one of the labeled probes. Membranes were then washed twice in hybridization buffer, and the relative abundance of mRNA was determined with a Fujix BAS 1000 phosphorimager. Nuclear run-on transcription assays were performed essentially according to published protocols (21). Briefly, MA104 cells (10⁸ cells/reaction) were harvested with a rubber policeman at different times postinfection, pelleted by centrifugation at 1,000 × g for 5 min, and washed twice in ice-cold phosphate-buffered saline. Cells were resuspended in 4 ml of lysis buffer (10 mM Tris HCl [pH 7.4], 10 mM NaCl, 3 mM MgCl₂, 0.5% Nonidet P-40) by gentle vortexing, and the nuclei were pelleted (1,000 × g for 5 min). The nuclei were stored in 100 µl of storage buffer (50 mM Tris HCl [pH 8.3], 40% glycerol, 5 mM MgCl₂, 0.1 mM EDTA) and frozen in liquid N₂. Labeled transcripts were prepared by incubating isolated nuclei in reaction buffer (final concentration: 10 mM Tris HCl [pH 8.0], 5 mM MgCl₂, 0.3 M KCl, 1 mM ATP, 1 mM CTP, 1 mM GTP, 1 mM DTT, 40 U of RNasin per ml), with 400 µCi of [α-³²P]UTP for 30 min at 37°C in a final volume of 200 µl. DNA was digested by the addition of RNase-free DNase (Boehringer Mannheim). Labeled RNA was extracted sequentially with guanadinium thiocyanate and phenol-chloroform and precipitated with isopropanol. RNA was resuspended in TES buffer [10 mM N-Tris (hydroxymethyl)methyl-2-aminoethanesulfonic acid (TES) (pH 7.4), 10 mM EDTA, 0.2% SDS], and aliquots of each sample were adjusted to 8 × 10⁸ cpm/ml by addition of TES buffer. One milliliter of RNA solution was mixed with 1 ml of TES–0.6 M NaCl, to which was added the appropriate cDNA immobilized to a nitrocellulose membrane (Schleicher & Schuell). Hybridization of the labeled RNA was performed over 36 h at 65°C, after which the nitrocellulose was washed twice in 25 ml of 2× SSC (1× SSC is 0.15 M NaCl plus 0.015 M sodium citrate) at 60°C for 30 min each—or under

more stringent conditions if necessary. The strips were then dried and analyzed by phosphorimaging or exposed to Kodak Hyperfilm.

RESULTS

Cellular protein expression is affected by rotavirus infection. Comparison of 2D protein maps prepared from ³⁵S-labeled MA104 cells reveals striking differences in the pattern of cellular protein expression following infection by rotavirus (Fig. 1A and B). The 2D protein map generated from infected cells is characterized by the presence of a large number of new proteins that are highly labeled (circled in Fig. 1B) and a general decrease in the labeling intensity of the majority of the other cellular proteins. This result was anticipated, because several previous studies have shown that rotavirus infection results in a dramatic decrease in the level of host cell translation and a high level of expression of viral polypeptides (6, 10). Forty-six new proteins were detected reproducibly in the infected-cell lysate when a matched set of scanned gel images was generated. The majority of these could be divided into three groups on the basis of molecular mass. For example, 11 new proteins that migrated with an apparent molecular mass of about 44 kDa were detected in virus-infected lysates, forming a string of protein spots with similar molecular masses but different pI's. All of these have been identified as VP6 by immunoblotting and/or mass spectrometry (data not shown). The presence of multiple VP6 isoforms in preparations of protein derived from purified virions has recently been demonstrated (9). A further 20 new proteins migrated between 25 and 30 kDa. Some of these were identified as NSP4 by comparison with immunoblotted 2D gels probed with anti-NSP4 antisera, and others were identified tentatively as NSP5 after labeling with ³²P (data not shown). A third group of new spots share a low molecular mass (<12 kDa) and are predominantly acidic. The identity of these is unknown, and it is possible that they represent degradation products of other viral proteins. The absence of new spots of higher molecular mass (e.g., VP1, VP2, etc.) probably reflects the failure of the viral inner core particles to denature and release their constituent polypeptides during the isoelectric focusing step (first dimension).

The matched set of gels was compared to identify cellular polypeptides whose expression was upregulated following rotavirus infection. Proteins in this category were identified by visual scanning, and they localized to two distinct regions of the gels. Three are acidic proteins in the molecular mass range 70 to 95 kDa (spots 1, 2, and 3, large rectangle, Fig 1B and C), and a fourth protein migrated with a similar molecular mass but was of a basic character (spot 8, small rectangle, Fig 1B and C). The relative increase in the level of expression of each polypeptide was determined by excision of the appropriate spot from the gel, elution of the labeled protein, and liquid scintillation counting (Fig. 1D). The abundance of the upregulated polypeptides increased between 1.7- and 2.6-fold following viral infection. In contrast, the abundance of six different cellular polypeptides decreased by a similar magnitude following rotavirus infection. This observation is further supported by several previous studies that report a decrease in host protein synthesis in rotavirus-infected cells (6, 10, 22). Thus the apparent two-fold increase in spots 1, 2, 3, and 8 should be viewed against the general trend in host cell protein synthesis, which exhibits an overall twofold decrease following rotavirus infection.

Identification of rotavirus-induced proteins. To identify the upregulated polypeptides, preparative gels were run, and proteins were detected by Coomassie blue staining. Only proteins in spots 2 and 3 were sufficiently abundant and well resolved after this procedure to permit their characterization by N-

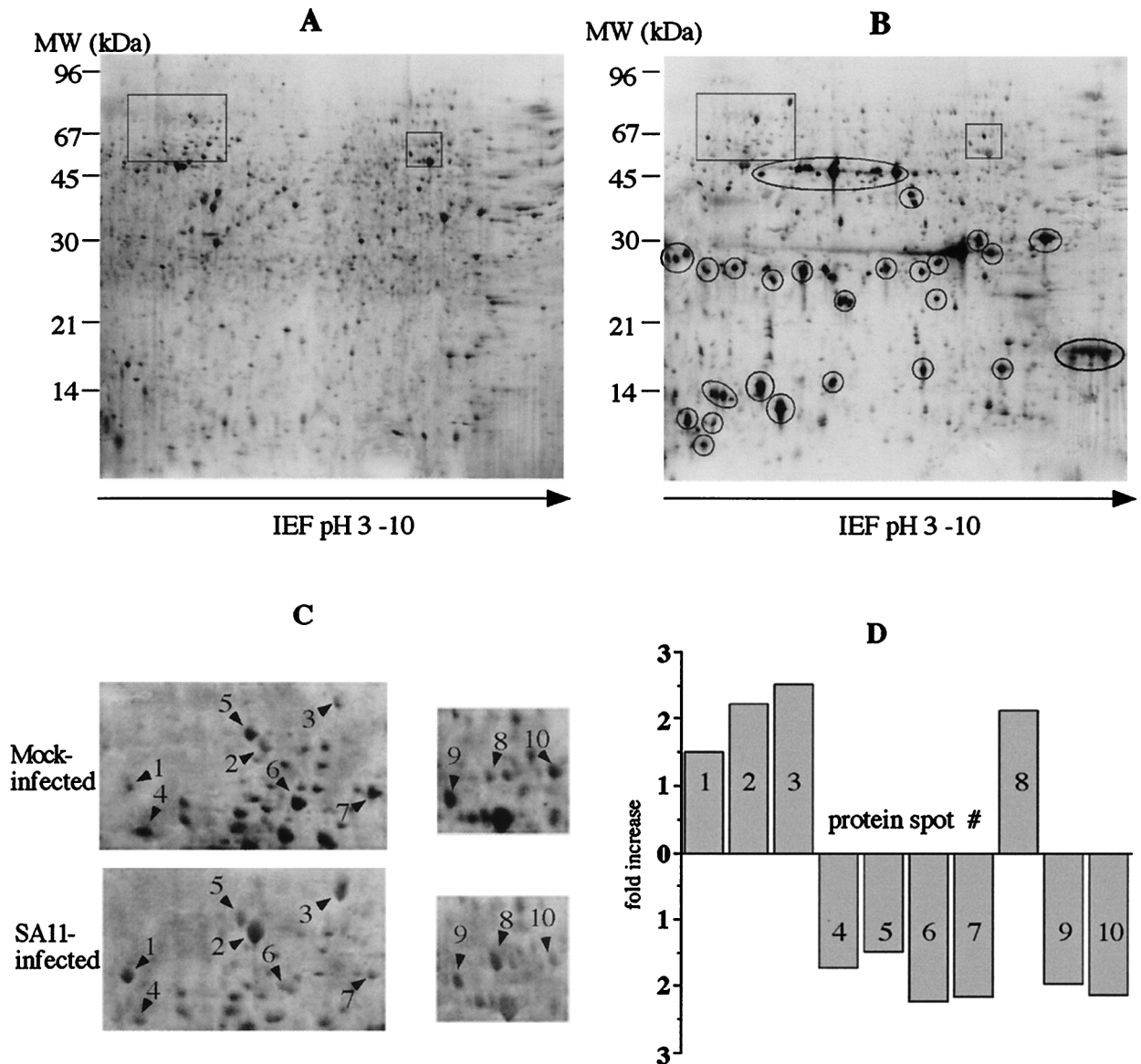


FIG. 1. 2D gel electrophoresis maps of protein from [^{35}S]Met- and [^{35}S]Cys-labeled MA10 cells either mock infected (A) or infected with 10 PFU of SA11 rotavirus per cell (B). The electrophoresis conditions were as described in Materials and Methods. Spots derived from virus-encoded proteins are circled. The large and small rectangles denote regions from each gel cell in which upregulated cellular proteins were detected. (C) Enlarged views of regions within the large and small rectangles from each gel showing the positions of a matched set of 10 polypeptides. (D) Increase or decrease in the amount of radioactivity associated with each of the marked spots from the virus-infected sample relative to those in the mock-infected control. MW, molecular mass.

terminal sequence analysis and peptide mass fingerprinting. These spots were excised from a total of eight preparative gels and subjected to in-gel trypsinization. The peptides were then eluted from the gel and purified by reverse-phase HPLC. From each digest, one well-resolved peptide was selected for N-terminal amino acid sequencing. The peptide from spot 2 yielded the N-terminal sequence VYEGERPL. Analysis of the Swiss-prot-PIR database (<http://www.expasy.hcuge.ch>) revealed 11 identical matches. Each match corresponded to residues 465 to 472 of the ER chaperone BiPs (GRP78) from various mammalian species. A similar analysis was performed for the sequence LGVIEDHS derived from spot 3. Twelve matches were found, each corresponding to endoplasmic (GRP94) from various mammalian species, all of which contain this sequence between residues 494 and 501. Like BiP, this protein

is also an ER-resident chaperone. To confirm the identity of the protein in each spot, the peptide mass fingerprint of a tryptic digest of each protein (Fig. 2) was compared to the sequence in the database by using the PeptideSearch program (accessed via <http://www.mann.embl-heidelberg.de/>). Matches were restricted to proteins with a molecular mass of between 30 and 200 kDa. At least seven peptides were required to match each database entry, with a peptide mass accuracy of 1 Da. Again BiP (spot 2) and endoplasmic (spot 3) were selected as the top matched proteins from the database (Table 1). Therefore, we conclude that the proteins in spots 2 and 3 correspond to BiP and endoplasmic, respectively.

Rotavirus infection increases mRNA steady-state abundance and transcriptional activity of the genes encoding BiP and endoplasmic. To determine whether the increase in BiP

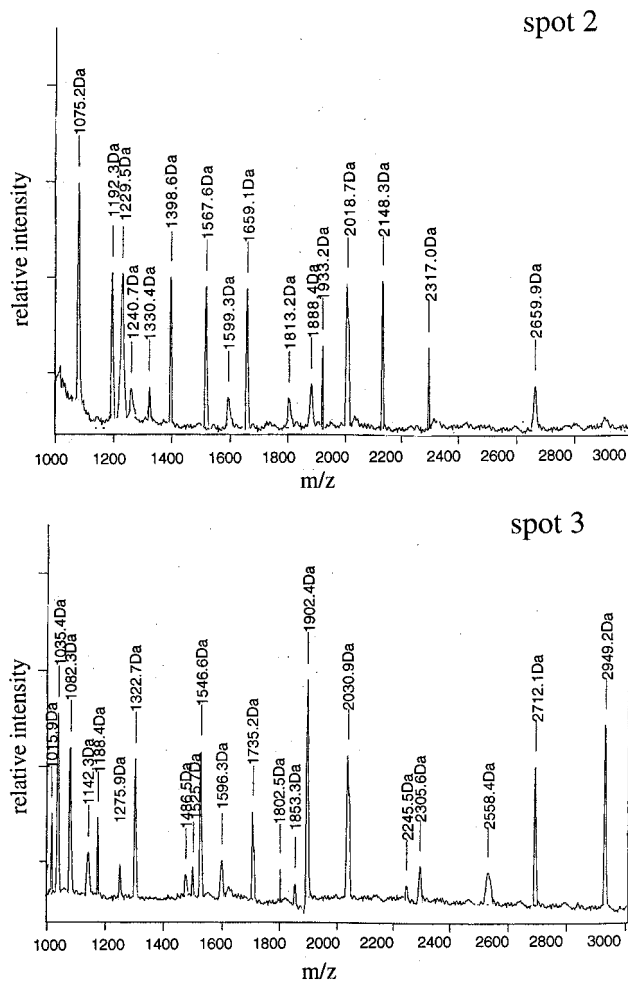


FIG. 2. Peptide mass fingerprint of a tryptic digest of the protein from spots 2 and 3. Only peptides in the mass range 1,000 to 3,000 Da were analyzed and used for mass matching with the database. All peaks represent the $M+H^+$ charge state.

and endoplasmic reticulum (ER) chaperone protein BiP. In contrast, endoplasmic reticulum chaperone protein BiP and endoplasmic reticulum chaperone protein BiP was due to transcriptional or posttranscriptional control, we investigated the kinetics of mRNA accumulation. RNA was prepared from mock-infected or SA11 rotavirus-infected MA104 cells at various times postinfection, and the levels of BiP and endoplasmic reticulum chaperone protein BiP mRNA were determined by Northern blotting (Fig. 3). mRNA extracted from reovirus-infected MA104 cells was also included as a further control. Levels of both BiP and endoplasmic reticulum chaperone protein BiP mRNA were increased markedly in rotavirus-infected cells from 7.5 h postinfection (hpi). In contrast, levels of glyceraldehyde 3-phosphate dehydrogenase (GAPDH) mRNA were unchanged during the first 10 h of infection. No change in the steady-state abundance of BiP or endoplasmic reticulum chaperone protein BiP mRNA was observed in either mock-infected cells or reovirus-infected cells.

Next, the transcriptional activity of the BiP and endoplasmic reticulum chaperone protein BiP genes was analyzed. Isolated nuclei prepared from rotavirus-infected MA104 cells were used for *in vitro* run-on transcription assays, and the levels of several mRNA species were determined. Figure 4 shows that the transcriptional activity of genes encoding both BiP and endoplasmic reticulum chaperone protein BiP is enhanced markedly at 5 h postinfection. This increase is maximal at 7.5 hpi (16- and 14-fold, respectively) and has declined slightly by 10 hpi (13- and 10-fold, respectively). In contrast, the rates of transcription of GAPDH and hsp70 are slightly decreased by 7.5 hpi (three- and fourfold, respectively).

NSP4 expression induces transcription of the BiP and endoplasmic reticulum chaperone protein BiP genes. We next considered whether induction of BiP and endoplasmic reticulum chaperone protein BiP required the assembly of virus in the infected cell, or whether one or more rotavirus gene products could specifically trigger the induction process. Both BiP and endoplasmic reticulum chaperone protein BiP are thought to have a molecular chaperone function within the ER and to act by preventing the misfolding and aggregation of proteins following a variety of conditions that result in ER stress (18). Any viral polypeptide that imparts stress to the ER might therefore cause induction of BiP and/or endoplasmic reticulum chaperone protein BiP. The nonstructural glycoprotein NSP4 is a likely candidate for such a role given (i) the localization of this protein to the ER membrane and (ii) the ability of this protein to increase intracellular calcium and perturb the ER membrane (36).

TABLE 1. Results of a database search for mass-matched peptides derived from tryptic digestion of proteins in spots 2 and 3

No. of matched peptides	Database accession no.	Protein name	Source	Molecular mass (kDa)
Spot 2				
11	swissprot:P06761	GRP78	Rat	72.35
11	swissprot:P20029	GRP78	Mouse	72.42
11	swissprot:P07823	GRP78	Hamster	72.38
11	trembl:D78645	GRP78	Mouse	72.46
10	swissprot:P11021	GRP78	Human	72.12
10	sptrembl:Q90593	GRP78	Chick	72.02
10	sptrembl:Q35642	BiP	Mouse	72.48
9	sptrembl:Q91883	BiP	Frog	72.64
8	sptrembl:Q31721	Pyruvate carboxylase ^a	<i>Bacillus subtilis</i>	127.71
8	sptremblnew:G282634	DNA polymerase ^a		191.71
Spot 3				
13	swissprot:P41148	Endoplasmic reticulum chaperone protein BiP	Dog	92.51
12	pir:S51358	ppk98	Pig	92.42
12	sptrembl:Q9070	GRP94	Pig	92.52
12	sptrembl:Q29091	ppk98	Pig	92.86
12	sptrembl:Q29092	ppk98	Pig	92.47
10	sptrembl:O16568	F40E12-2 ^a	<i>Caenorhabditis elegans</i>	142.85
10	swissprot:P08113	Endoplasmic reticulum chaperone protein BiP	Mouse	92.48
9	sptrembl:Q90869	hsp108	Chick	91.28
9	swissprot:P08110	Endoplasmic reticulum chaperone protein BiP	Chick	91.56
9	swissprot:P14625	Endoplasmic reticulum chaperone protein BiP	Human	92.47

^a Protein discarded as a potential match because the molecular mass was significantly different from that apparent for spots 2 and 3 from the 2D gels.

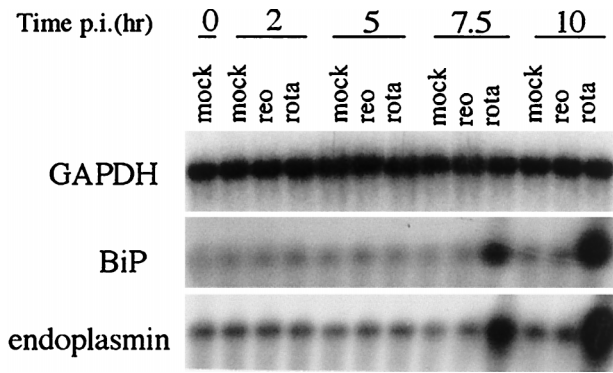
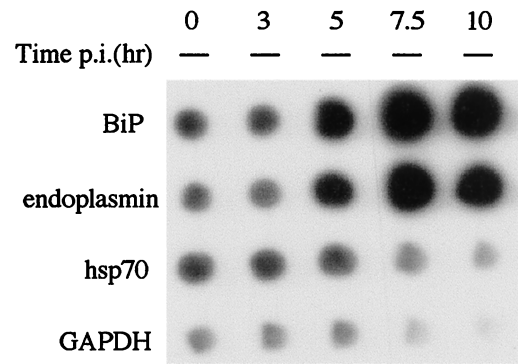


FIG. 3. Rotavirus infection increases BiP and endoplasmin mRNA abundance in MA104 cells. mRNA levels were analyzed at 2, 5, 7.5, and 10 hpi. At each time point, RNA was extracted from mock-infected cells (mock), reovirus-infected cells (reo), and rotavirus-infected cells (rota) and resolved by electrophoresis. The membranes were then probed for the abundance of mRNA encoding BiP, endoplasmin, and GAPDH. For further details, see Materials and Methods.

A dual vaccinia virus recombinant expression system was employed to express NSP4 in MA104 cells at a level comparable to that observed during rotavirus infection (28). Cells were infected either with 20 PFU of vTF7-3, a recombinant vaccinia virus that expresses T7 RNA polymerase, per cell or 10 PFU of vTF7-3 plus 10 PFU of vTMNSP4 per cell, which leads to expression of NSP4 under the transcriptional control of the bacteriophage T7 promoter (8, 12). Northern blotting was performed to measure the mRNA steady-state abundance of BiP, endoplasmin, and an unrelated mRNA species GAPDH at 8 and 12 hpi. The level of all three mRNA species decreased three- to fourfold in cells infected with 20 PFU of vTF7-3 per cell relative to mock-infected cells (data not shown), consistent with previous reports that vaccinia virus infection causes a general degradation of host cell mRNA (33). In contrast, levels of BiP and endoplasmin mRNA exhibited little change in cells infected with both vTF7-3 and vTMNSP4, although the level of GAPDH mRNA was again three- to fourfold lower than that in mock-infected cells (data not shown). Less equivocal were results obtained from nuclear run-on transcription assays (Fig. 5). These show that expression of NSP4 results in an increase in the rate of transcription of the genes encoding BiP and endoplasmin. Transcription of BiP mRNA was increased 3.8- and 3.4-fold over that in control cells infected with vTF7-3 at 8 and 12 hpi, respectively, while transcription of endoplasmin was increased 4.8- and 4.1-fold at these times. Transcription of hsp70 mRNA increased two- to threefold in response to vTF7-3 or the vTF7-3-vTMNSP4 combination. Activation of hsp70 transcription by vaccinia viruses has previously been reported (13). The rate of GAPDH transcription was unchanged.

Association of rotavirus protein with BiP and endoplasmin.

Both BiP and endoplasmin have been shown to associate with certain newly synthesized, unfolded, or misfolded polypeptides (20, 27). Moreover, several studies have shown that association of polypeptides with BiP or endoplasmin is accompanied by the transcriptional upregulation of these genes (14, 31, 39). Therefore, we investigated whether BiP or endoplasmin was associated with any rotavirus proteins during infection. Given the ability of NSP4 to induce the transcription of these genes, we tested whether this might reflect the association of NSP4 with either BiP or endoplasmin. MA104 cells were prelabeled for 24 h prior to infection with either vTF7-3 or a combination of vTF7-3 and vTMNSP4. At 7 hpi, the cells were given a 10-min pulse with ³⁵S and either lysed immediately or chased in



BiP	1	1	3	16	14
endoplasmin	1	1	4	13	10
hsp70	1	1	1	-3	-4
GAPDH	1	1	1	-2	-5

FIG. 4. Transcriptional activation of genes encoding BiP and endoplasmin following rotavirus infection. Nuclei were isolated from rotavirus-infected MA104 cells at the indicated times and used for run-on transcription assays in the presence of [α -³²P]UTP as described in Materials and Methods. Labeled RNA was purified and hybridized to nitrocellulose strips containing probes for BiP, endoplasmin, hsp70, and GAPDH. Bound RNA was quantified by analysis in a Fuji phosphorimager. The increase in each mRNA species relative to the initial amount is illustrated in the attached table. Note that negative values indicate a decrease.

unlabeled medium for different intervals and then lysed. Cells were lysed in non-denaturing buffer to limit disruption of weakly interacting protein complexes. Lysates were then immunoprecipitated, either with a monoclonal antibody against NSP4, or with a polyclonal serum against the carboxy-terminal portion of endoplasmin—which cross-reacts with BiP. Immediately after labeling, NSP4 in various states of glycosylation was precipitated by the anti-NSP4 monoclonal antibody (Fig. 6, lane 1). After a short chase period, only a single 28-kDa species, representing the diglycosylated form of NSP4, was

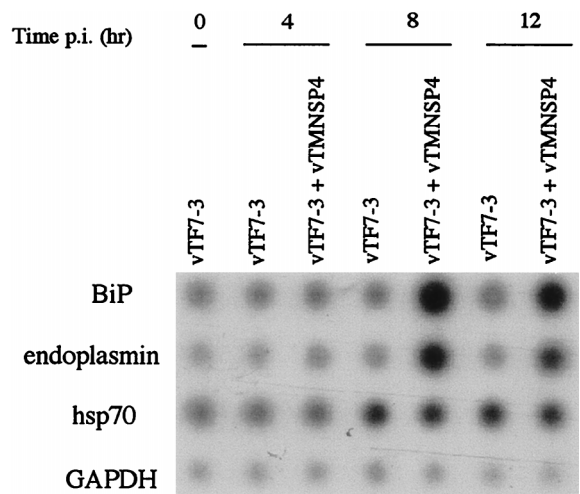


FIG. 5. Expression of NSP4 enhances the transcription of genes encoding BiP and endoplasmin. Nuclei were isolated from MA104 cells infected with either 20 PFU of vTF7.3 per cell or 10 PFU of vTF7.3 plus 10 PFU of vTMNSP4 per cell and used in run-on transcription assays as described in Materials and Methods. The presence of mRNA species encoding BiP, endoplasmin, hsp70, and GAPDH was determined with the corresponding probes at 4, 8, and 12 hpi.

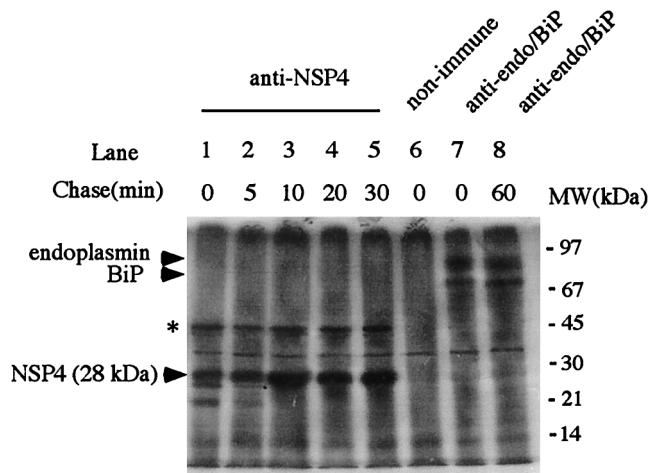


FIG. 6. NSP4 does not associate with BiP or endoplasmic reticulum. MA104 cells were labeled for 24 h with ^{35}S -Trans-label prior to infection with 10 PFU of vTF7.3 plus 10 PFU of vTMNSP4 per cell and thereafter grown in unlabeled medium. At 7 hpi, cells were pulse-labeled for 10 min and then chased for the indicated times, after which the cells were lysed and proteins were immunoprecipitated with either a monoclonal antiserum against NSP4 (lanes 1 to 5) or a polyclonal antiserum against endoplasmic reticulum that cross-reacts with BiP (lanes 7 and 8). The asterisk denotes the position of an unidentified cellular protein that coprecipitated with NSP4. MW, molecular mass.

evident. Antibodies against BiP and endoplasmic reticulum precipitated both proteins as well as a further 36-kDa band that was common to both sera and thus deemed to be nonspecific (Fig. 6, lanes 7 and 8). No evidence was found for association between NSP4 and either BiP or endoplasmic reticulum.

We next investigated whether any of the rotavirus structural polypeptides were associated with either of the upregulated chaperones. Cells were infected with SA11 rotavirus and were pulse-labeled at 7 hpi and chased for periods of up to 2 h. As anticipated, a polyclonal antiserum against rotavirus particles efficiently precipitated the structural polypeptides from the infected-cell lysates (Fig. 7, lanes 1 and 2). Remarkably, most of the rotavirus structural proteins were also precipitated by antibodies against endoplasmic reticulum, suggesting that endoplasmic reticulum and/or BiP associates with a virion component in the ER during assembly. Immediately after labeling, the proportions of VP4 and VP7 precipitated by the antiendoplasmic reticulum serum were 15 and 20%, respectively, of that precipitated by the antirotavirus antibody. The relative proportions increased to 47 and 56%, respectively, after a 30-min chase and thereafter decreased with time. In contrast, the proportion of the total radioactivity associated with VP2 and VP3 (13%) and VP6 (9%) that was precipitated by antiendoplasmic reticulum antibody relative to the amount precipitated by antirotavirus antiserum was unchanged throughout the experiment. A small but significant amount of virus remained associated with BiP and endoplasmic reticulum even after 2 h (Fig. 7, lane 7). In a parallel immunoprecipitation experiment, both BiP and endoplasmic reticulum were efficiently recovered from lysates of cells prelabeled for 16 h prior to infection, both with anti-endoplasmic reticulum (lane 9) and anti-SA11 rotavirus (lane 10) antibodies, but not with a nonimmune rabbit serum (lane 11). This observation suggests that both BiP and endoplasmic reticulum are associated with virion components within the ER.

DISCUSSION

Refinement of methods for the resolution of protein mixtures by 2D gel electrophoresis has enabled the analysis of

protein expression in a variety of cells and tissues. The ability to map the total complement of proteins expressed in a given cell (referred to as the "proteome") enables the establishment of a reference against which alterations in the pattern of protein expression following virus infection may be determined. When applied to the analysis of MA104 cells infected with rotavirus, the most striking feature of the proteome maps is the appearance of many new virus-encoded proteins (compare Fig. 1A and B). Surprisingly, although rotavirus encodes only 11 proteins, a total of 46 highly labeled new spots were evident in the map derived from virus-infected cells. Our data suggest that many rotavirus proteins exist in multiple isoforms, possibly reflecting differences in the extent of posttranslational modification. In support of this notion, a previous analysis of NSP5 by 2D polyacrylamide gel electrophoresis revealed the existence of several isoforms that differed in molecular mass and pI and which were also labeled with ^{32}P , suggesting that this protein is phosphorylated at several sites (4). In this study, immunoblotting of the gels with antisera against VP6 and NSP4 demonstrated that these proteins also exist in multiple states (data not shown). 2D gel electrophoresis and mass spectrometry analysis of VP6 from purified virions have also revealed a level of heterogeneity similar to that observed in this study (9).

The majority of host cell proteins were expressed at a level approximately two- to threefold less than that in mock-infected cells. However, careful analysis of the gels revealed four proteins that increased in abundance following virus infection. Limitations to the resolution of the total proteome in a single 2D gel mean that it is possible that the number of upregulated host cell proteins is greater. We are currently refining the conditions of electrophoresis to expand the resolution in selective regions of the gels and analyzing subcellular fractions of infected MA104 cells. Together these approaches should yield more informative data about the effect of virus infection on host cell protein expression.

Two upregulated proteins were identified as BiP and endoplasmic reticulum (also known as glucose-regulated proteins GRP78 and GRP94, respectively). Northern analysis and nuclear run-on transcription assays clearly demonstrate that a marked increase in transcription accounts for the upregulation of BiP and endoplasmic reticulum in rotavirus-infected cells. These proteins

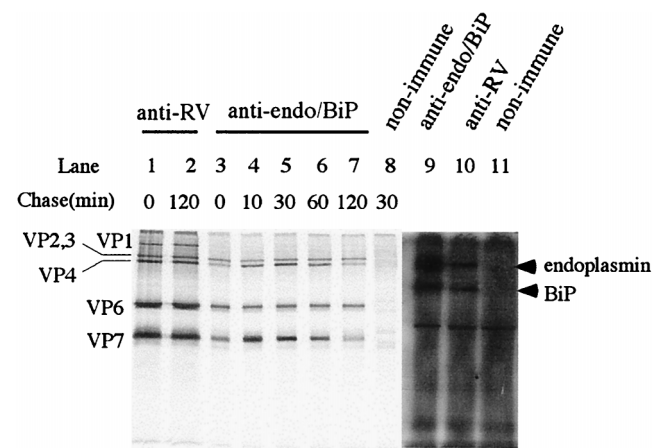


FIG. 7. BiP and endoplasmic reticulum bind to rotavirus (RV) structural polypeptides during virion maturation in the ER. Rotavirus-infected MA104 cells were pulse-labeled at 7 hpi and chased for the indicated times. The cells were lysed and the proteins were immunoprecipitated with either anti-SA11 rotavirus, antiendoplasmic reticulum antiserum, or nonimmune serum (lanes 1 to 8). Alternatively, cells were labeled for 16 h with ^{35}S -Trans-label, chased for 1 h before infection, and immunoprecipitated 7 hpi (lanes 9 to 11).

function as ER-resident molecular chaperones that assist in the folding and oligomerization of proteins within the ER lumen. The induction of BiP and endoplasmic reticulum chaperone (ER) is believed to protect cells from a variety of external and internal stimuli that exhibit, as a common feature, the potential to induce stress within the ER lumen and therefore lead to the accumulation of misfolded proteins (reviewed in reference 18). A variety of pharmacological agents, such as the Ca^{2+} ionophore A23187 and thapsigargin (an inhibitor of the ER Ca^{2+} ATPase), lead to a reduction in ER Ca^{2+} levels (16, 32). It has been suggested that this reduction in ER Ca^{2+} impairs normal protein folding in the ER, and thus increased BiP is required to prevent protein aggregation (19). Similarly, internal stimuli such as the expression of folding-incompetent mutant polypeptides or high-level expression of complex oligomeric proteins, require an increase in BiP levels to prevent the aggregation of protein within the organelle (27). Virus infection can also lead to the induction of such a stress within the ER. For example, infection with the paramyxovirus simian virus 5 (SV5) causes an increase in synthesis of BiP (29). The expression of the SV5 hemagglutinin-neuraminidase (HN) protein alone was sufficient to promote induction of BiP, suggesting that proteins whose folding and oligomerization proceed more slowly, as evidenced by a prolonged association with BiP, may require increased levels of this chaperone (39).

NSP4 is localized to the ER membrane and has been reported to possess membrane-destabilizing activity (36). Therefore, we reasoned that its expression may be sufficient to cause the induction of BiP and endoplasmic reticulum chaperone. Delivery of NSP4 via a recombinant vaccinia virus vector resulted in a three- to four-fold increase in BiP and endoplasmic reticulum chaperone transcription over vaccinia virus-infected control cells. We could not detect any association between NSP4 and either BiP or endoplasmic reticulum chaperone in coimmunoprecipitation experiments (Fig. 5). This result was not unexpected, because only a small portion of the N terminus of NSP4 is believed to project into the ER lumen (3, 7). We conclude that the ability of NSP4 to induce transcription of the BiP and endoplasmic reticulum chaperone genes derives not from its own folding requirements, but rather from its effects on the integrity of the ER, possibly by contributing to the reduction in the luminal Ca^{2+} concentration as a result of the disruption of the ER membrane. Michelangeli et al. have suggested that a high ER Ca^{2+} concentration is required for the productive maturation of rotavirus in this organelle (24). It is interesting to note that BiP has recently been assigned a Ca^{2+} storage role and contributes ~25% of the exchangeable Ca^{2+} pool within the ER (17). We hypothesize that a depletion of the ER Ca^{2+} pool in response to NSP4 expression may partially be offset by upregulation of BiP expression and its recruitment to the ER lumen—where it may function to prevent protein aggregation and restore Ca^{2+} homeostasis within this compartment.

BiP and endoplasmic reticulum chaperone may also participate in the folding of the rotavirus outer capsid proteins during assembly of virions within the ER. Antibodies against endoplasmic reticulum chaperone which cross-react with BiP efficiently precipitated the rotavirus structural proteins from lysates of infected cells (Fig. 6). The proportion of VP4 and VP7 that was bound to BiP or endoplasmic reticulum chaperone increased immediately following their synthesis, reaching a maximum after 30 min. A proportion of the rotavirus structural proteins could still be coimmunoprecipitated with antiendoplasmic reticulum chaperone 2 h after their synthesis (Fig. 6, lane 7). Recently VP7 has been shown to associate with another ER-localized chaperone, protein disulfide isomerase (PDI) (26). The kinetics of the VP7-PDI interaction showed a maximal association after 120 min. As rotavirus particles assemble in the ER, they might interact sequentially with several different

chaperone proteins until the mature virions are completely assembled and can be released. The fact that an antirotavirus antibody precipitated both BiP and endoplasmic reticulum chaperone from prelabeled infected cells suggests that both chaperones are involved in the folding and assembly process and thus may function in concert.

In summary, by applying a proteome-mapping approach to the analysis of rotavirus-infected cells, we have identified BiP and endoplasmic reticulum chaperone as two proteins whose synthesis is upregulated postinfection. A further two proteins remain to be identified from our initial 2D gel analysis. The roles of these and other host proteins in the assembly and pathology of rotavirus infection remain to be established.

ACKNOWLEDGMENTS

We thank Harry Greenberg for providing a monoclonal antibody specific for NSP4. Amy Lee provided plasmids p4A3 and pBC5, and Michael Green provided antiendoplasmic reticulum chaperone antiserum. We are grateful to Garth Cooper for access to 2D electrophoresis and mass spectrometry facilities.

This work was supported by a project grant from the Health Research Council of New Zealand.

REFERENCES

1. Au, K.-S., W.-K. Chan, J. W. Burns, and M. K. Estes. 1989. Receptor activity of rotavirus nonstructural glycoprotein NS28. *J. Virol.* **63**:4553–4562.
2. Ball, J. M., P. Tian, C. W.-Y. Zeng, A. P. Morris, and M. K. Estes. 1996. Age-dependent diarrhea induced by a rotaviral nonstructural glycoprotein. *Science* **272**:101–104.
3. Bergmann, C. C., D. Maass, M. K. Poruchynsky, P. H. Atkinson, and A. R. Bellamy. 1989. Topology of the non-structural rotavirus receptor glycoprotein NS28 in the rough endoplasmic reticulum. *EMBO J.* **8**:1695–1703.
4. Blackhall, J., A. Fuentes, K. Hansen, and G. Magnusson. 1997. Serine protein kinase activity associated with rotavirus phosphoprotein NSP5. *J. Virol.* **71**:138–144.
5. Both, G. W., L. J. Siegman, A. R. Bellamy, and P. H. Atkinson. 1983. Coding assignment and nucleotide sequence of simian rotavirus SA11 gene segment 10: location of glycosylation sites suggests that the signal peptide is not cleaved. *J. Virol.* **48**:335–339.
6. Carpio, M. M., L. A. Babiuik, V. Misra, and R. M. Blumenthal. 1981. Bovine rotavirus interactions: effect of virus infection on cellular integrity and macromolecular synthesis. *Virology* **114**:86–97.
7. Chan, W. K., K. S. Au, and M. K. Estes. 1988. Topography of the simian rotavirus nonstructural glycoprotein (NS28) in the endoplasmic reticulum membrane. *Virology* **164**:435–442.
8. Elroy-Stein, O. T., T. Fuerst, and B. Moss. 1989. Cap-independent translation of mRNA conferred by encephalomyocarditis virus 5' sequence improves the performance of the vaccinia virus/bacteriophage T7 hybrid expression system. *Proc. Natl. Acad. Sci. USA* **86**:6126–6130.
9. Emslie, K. R., M. P. Molloy, C. R. M. Baradil, D. Jardine, M. R. Wilkins, A. R. Bellamy, and K. L. Williams. Characterisation of the rotavirus SA11 VP6 protein using mass spectrometry and two-dimensional gel electrophoresis. Submitted for publication.
10. Ericson, B. L., D. Y. Graham, B. B. Mason, and M. K. Estes. 1982. Identification, synthesis, and modifications of simian rotavirus SA11 polypeptides in infected cells. *J. Virol.* **42**:825–839.
11. Estes, M. K. 1995. Rotaviruses and their replication, p. 731–761. *In* B. N. Fields, D. Knipe, P. M. Howley, et al. (ed.), *Fields virology*, 3rd ed. Lippincott-Raven Publishers, Philadelphia, Pa.
12. Fuerst, T. R., P. L. Earl, and B. Moss. 1987. Use of a hybrid vaccinia virus-T7 RNA polymerase system for expression of target genes. *Mol. Cell. Biol.* **7**:2538–2544.
13. Jindal, S., and R. A. Young. 1992. Vaccinia virus infection induces a stress response that leads to association of Hsp70 with viral proteins. *J. Virol.* **66**:5357–5362.
14. Kozutsumi, Y. M., M. Segal, K. Normington, M.-J. Gething, and J. Sambrook. 1988. The presence of misfolded proteins in the endoplasmic reticulum signals the induction of glucose regulated proteins. *Nature (London)* **332**:462–464.
15. Lee, A. S., A. Delegeane, and D. Scharf. 1981. Highly conserved glucose-regulated protein in hamster and chicken cells: preliminary characterization of its cDNA clone. *Proc. Natl. Acad. Sci. USA* **78**:4922–4925.
16. Li, W. W., S. Alexandre, X. Cao, and A. S. Lee. 1993. Transactivation of the grp78 promoter by Ca^{2+} depletion. *J. Biol. Chem.* **268**:12003–12009.
17. Lievreumont, J.-P., R. Rizzuto, L. Hendershot, and J. Meldolesi. 1997. BiP, a major chaperone of the endoplasmic reticulum lumen, plays a direct and

- important role in the storage of the rapidly exchanging pool of Ca^{2+} . *J. Biol. Chem.* **272**:30873–30879.
18. Little, E., M. Ramakrishnan, B. Roy, G. Gazit, and A. S. Lee. 1994. The glucose regulated proteins (GRP 78 and GRP94): function, gene regulation and applications. *Crit. Rev. Eukaryot. Gene Expr.* **4**:1–18.
 19. Lodish, H. F., and N. Kong. 1990. Perturbation of cellular calcium blocks exit of secretory proteins from the rough endoplasmic reticulum. *J. Biol. Chem.* **265**:10893–10899.
 20. Machamer, C. E., R. W. Doms, D. G. Bole, A. Helenius, and J. K. Rose. 1990. Heavy chain binding protein recognizes incompletely disulphide-bonded forms of vesicular stomatitis virus G protein. *J. Biol. Chem.* **263**:2107–2110.
 21. McCormick, T. S., K. S. McColl, and C. W. Distelhorst. 1997. Mouse lymphoma cells destined to undergo apoptosis in response to thapsigargin treatment fail to generate a calcium-mediated grp78/grp94 stress response. *J. Biol. Chem.* **272**:6087–6092.
 22. McCrae, M. A., and G. P. Faulkener-Valle. 1981. Molecular biology of rotaviruses. I. Characterization of basic growth parameters and pattern of macromolecular synthesis. *J. Virol.* **39**:490–496.
 23. Meyer, J. C., C. C. Bergmann, and A. R. Bellamy. 1989. Interaction of rotavirus cores with the nonstructural glycoprotein NS28. *Virology* **171**:98–107.
 24. Michelangeli, F., F. Liprandi, M. E. Chemello, M. Ciarlet, and M.-C. Ruiz. 1995. Selective depletion of calcium by thapsigargin blocks rotavirus maturation but not the cytopathic effect. *J. Virol.* **69**:3838–3847.
 25. Michelangeli, F., M.-C. Ruiz, J. R. del Castillo, J. E. Ludert, and F. Liprandi. 1991. Effect of rotavirus infection on intracellular calcium homeostasis in cultured cells. *Virology* **181**:520–527.
 26. Mirazimi, A., and L. Svensson. 1998. Carbohydrates facilitate correct disulfide bond formation and folding of rotavirus VP7. *J. Virol.* **72**:3887–3892.
 27. Navarro, D., I. Quadri, and L. Pereira. 1991. A mutation in the ectodomain of herpes simplex virus 1 glycoprotein B causes defective processing and retention in the ER. *Virology* **180**:135–143.
 28. Newton, K., J. C. Meyer, A. R. Bellamy, and J. A. Taylor. 1997. Rotavirus nonstructural glycoprotein NSP4 alters plasma membrane permeability in mammalian cells. *J. Virol.* **71**:9458–9465.
 29. Peluso, R. W., R. A. Lamb, and P. W. Choppin. 1978. Infection with paramyxoviruses stimulates synthesis of cellular polypeptides that are also stimulated in cells transformed by Rous sarcoma virus or deprived of glucose. *Proc. Natl. Acad. Sci. USA* **75**:6120–6124.
 30. Poruchynsky, M. S., D. R. Maass, and P. H. Atkinson. 1991. Calcium depletion blocks the maturation of rotavirus by altering the oligomerization of virus-encoded proteins in the ER. *J. Cell Biol.* **114**:651–661.
 31. Ramakrishnan, M., S. Tugizov, L. Pereira, and A. S. Lee. 1995. Conformation-defective herpes simplex virus 1 glycoprotein B activates the promoter of the grp94 gene that codes for a 94 kDa stress protein in the endoplasmic reticulum. *DNA Cell Biol.* **14**:373–384.
 32. Resendez, E., Jr., J. W. Attenello, A. Graftsky, C. S. Chang, and A. S. Lee. 1985. Calcium ionophore A23187 induces expression of glucose-regulated genes and their heterologous fusion genes. *Mol. Cell. Biol.* **5**:1212–1219.
 33. Rice, A. P., and B. E. Roberts. 1983. Vaccinia virus induces cellular mRNA degradation. *J. Virol.* **47**:529–539.
 34. Rosenfield, T., J. Capedevielle, J. Guillemot, and P. Ferrara. 1992. In-gel digestion of proteins for internal sequence analysis after one or two gel electrophoresis. *Anal. Biochem.* **203**:173–179.
 35. Street, J. E., M. C. Croxson, W. F. Chadderton, and A. R. Bellamy. 1982. Sequence diversity of human rotavirus strains investigated by Northern blot hybridization analysis. *J. Virol.* **43**:369–378.
 36. Tian, P., J. M. Ball, C. Q. Y. Zeng, and M. K. Estes. 1996. The rotavirus nonstructural glycoprotein NSP4 possesses membrane destabilization activity. *J. Virol.* **70**:6973–6981.
 37. Tian, P., Y. Hu, W. P. Schilling, D. A. Lindsay, J. Eiden, and M. K. Estes. 1994. The nonstructural glycoprotein of rotavirus affects intracellular calcium levels. *J. Virol.* **68**:251–257.
 38. Tian, P., M. K. Estes, Y. Hu, J. M. Ball, C. Q.-Y. Zeng, and W. P. Schilling. 1995. The rotavirus nonstructural glycoprotein NSP4 mobilizes Ca^{2+} from the endoplasmic reticulum. *J. Virol.* **69**:5763–5772.
 39. Watowich, S. S., R. I. Moromoto, and R. A. Lamb. 1992. Flux of the paramyxovirus hemagglutinin-neuraminidase glycoprotein through the endoplasmic reticulum activates transcription of the *GRP78-BiP* gene. *J. Virol.* **65**:3590–3597.